Curse of Dimensionality on Randomized Smoothing for Certifiable Robustness

Aounon Kumar[1] **Alexander Levine**[1] **Tom Goldstein**[1] **Soheil Feizi**[1]

Abstract

Randomized smoothing, using just a simple isotropic Gaussian distribution, has been shown to produce good robustness guarantees against ℓ_2-norm bounded adversaries. In this work, we show that extending the smoothing technique to defend against other attack models can be challenging, especially in the high-dimensional regime. In particular, for a vast class of i.i.d. smoothing distributions, we prove that the largest ℓ_p-radius that can be certified decreases as $O(1/d^{\frac{1}{2}-\frac{1}{p}})$ with dimension d for $p > 2$. Notably, for $p \geq 2$, this dependence on d is no better than that of the ℓ_p-radius that can be certified using isotropic Gaussian smoothing, essentially putting a matching lower bound on the robustness radius. When restricted to *generalized* Gaussian smoothing, these two bounds can be shown to be within a constant factor of each other in an asymptotic sense, establishing that Gaussian smoothing provides the best possible results, up to a constant factor, when $p \geq 2$. We present experimental results on CIFAR to validate our theory. For other smoothing distributions, such as, a uniform distribution within an ℓ_1 or an ℓ_∞-norm ball, we show upper bounds of the form $O(1/d)$ and $O(1/d^{1-\frac{1}{p}})$ respectively, which have an even worse dependence on d.

1. Introduction

Deep neural networks, especially in image classification tasks, have been shown to be vulnerable to adversarial perturbations of the input that are unnoticeable to a human observer but can alter the prediction of the model (Szegedy et al., 2014). These examples are generated by optimizing a loss function for a trained network over the input features within a small neighborhood of an example input. Gradient

based methods such as FGSM (Goodfellow et al., 2015) and projected gradient descent (Madry et al., 2018) have been shown to be very effective for this purpose. In the last couple of years, several heuristic methods have been proposed to detect and/or defend against attacks from specific types of adversaries (Buckman et al., 2018; Guo et al., 2018; Dhillon et al., 2018; Li & Li, 2017; Grosse et al., 2017; Gong et al., 2017). Such defenses, however, have been shown to break down against more powerful attacks (Carlini & Wagner, 2017; Athalye et al., 2018; Uesato et al., 2018; Laidlaw & Feizi, 2019). For certain types of problems, adversarial examples might even be unavoidable (Shafahi et al., 2019).

This necessitates developing classifiers with robustness guarantees. Several convex relaxation-based techniques have been proposed to design *certifiably robust* classifiers (Wong & Kolter, 2018; Raghunathan et al., 2018; Singla & Feizi, 2019; Chiang et al., 2020; Singla & Feizi, 2020) whose predictions are guaranteed to remain constant within a certified neighborhood around the input point, thereby eliminating the presence of any adversarial example in that region. However, the ever-increasing complexity of deep neural networks has made it difficult to scale these methods meaningfully to high-dimensional datasets like ImageNet.

To deal with the scalability issue in certifiable robustness, a line of work has been introduced based on *randomized robustness* (Lécuyer et al., 2019; Li et al., 2019; Cohen et al., 2019; Salman et al., 2019; Levine & Feizi, 2020a;b;c; Lee et al., 2019; Teng et al., 2020; Zhang et al., 2020) wherein an arbitrary base classifier is made more robust by averaging its prediction over random perturbations of the input point within its neighborhood. Cohen et al. (2019) proved the first tight robustness guarantee for Gaussian smoothing for an ℓ_2-norm bounded adversary.

In this work, however, we show that extending the smoothing technique to defend against higher-norm attacks, especially in the high-dimensional regime, can be challenging. In particular, for a general class of i.i.d. smoothing distributions, we show that, for $p > 2$, the largest ℓ_p-radius that can be certified (denoted by r_p) decreases with the number of dimensions d as $O(1/d^{\frac{1}{2}-\frac{1}{p}})$. Note that the special case of $p = 2$ does not suffer from such dependency on d. This makes smoothing-based robustness bounds weak against ℓ_p adversarial attacks for large p, especially, for ℓ_∞ because as

---

[1]University of Maryland, College Park, Maryland, USA. Correspondence to: Aounon Kumar <aounon@umd.edu>, Soheil Feizi <sfeizi@cs.umd.edu>.

$p \to \infty$ the dependence on d becomes $O(1/\sqrt{d})$. Moreover, we show that the dependence of the robustness certificate on d using a general i.i.d. smoothing distribution is similar to that of the standard Gaussian smoothing, even for $p > 2$. This implies that Gaussian smoothing essentially provides the best possible robustness certificate result in terms of the dependence on d even for $p > 2$.

To be more precise, suppose we smooth a classifier by randomly sampling points surrounding an image x, and observing the labels assigned to these points. Let $p_1(x)$ and $p_2(x)$ be the probabilities of the first and second most probable labels under the smoothing distribution. We prove the following bounds on the robustness certificate:

1. When points are sampled by adding i.i.d. noise to each dimension in x with σ^2 variance and continuous support, we prove the certified ℓ_p radius bound

   $$r_p^* \leq \frac{\sigma}{2\sqrt{2}d^{\frac{1}{2}-\frac{1}{p}}} \left(\frac{1}{\sqrt{1-p_1(x)}} + \frac{1}{\sqrt{p_2(x)}} \right),$$

   whenever $p_1(x) \geq 1/2$. See Theorem 1.

2. When smoothing with a generalized Gaussian distribution with variance σ^2 (which includes Laplacian, Gaussian, and uniform distributions), we prove that

   $$r_p^* \leq \frac{2\sigma}{d^{\frac{1}{2}-\frac{1}{p}}} \left(\sqrt{\log \frac{1}{1-p_1(x)}} + \sqrt{\log \frac{1}{p_2(x)}} \right),$$

   when $e^{-d/4} < p_2(x) \leq p_1(x) < 1 - e^{-d/4}$. When d is large, these bounds do not impact the range of values that $p_1(x)$ and $p_2(x)$ can take in a significant way. See Theorem 2.

3. We also study smoothing techniques where the distribution is uniform over a region around the input point. When smoothed over an ℓ_∞ ball of radius b, i.e. uniform i.i.d between $-b$ and b in each dimension, we show that

   $$r_p^* < \frac{2b}{d^{1-\frac{1}{p}}} = 2\sqrt{3}\sigma/d^{1-\frac{1}{p}},$$

   where $\sigma^2 = b^2/3$ is the variance in each dimension. See Theorem 4. Note that this bound is independent of $p_1(x)$ and $p_2(x)$.

4. For smoothing uniformly over an ℓ_1 ball of the same radius b, we achieve an even stronger bound:

   $$r_p^* < \frac{2b}{d}$$

   See Theorem 5 for details. Along with being independent of $p_1(x)$ and $p_2(x)$, it is also independent of p.

Thus, it holds for any p-norm bounded adversary. Note that, unlike the other smoothing distributions we have considered, the uniform ℓ_1 smoothing is not i.i.d. in every dimension.

These bounds hold for any $p > 0$, but are too weak to offer meaningful insights when $p < 2$ in the first two cases and for $p < 1$ in the third one. Moreover, it is straightforward to show that, for $p \geq 2$, the following ℓ_p-radius can be certified using Cohen et al.'s (2019) Gaussian smoothing:

$$r_p = \frac{\sigma}{2d^{\frac{1}{2}-\frac{1}{p}}} \left(\Phi^{-1}\left(p_1(x)\right) - \Phi^{-1}\left(p_2(x)\right) \right), \quad (1)$$

which has the same dependence on d as the upper bound obtained using i.i.d. smoothing. This radius is asymptotically only a constant factor away from the upper bound for the generalized Gaussian distribution, showing that this family of distributions fails to outperform standard Gaussian smoothing in high dimensions. To the best of our knowledge, these bounds form the first results on the limitations of randomized smoothing in the high dimensional regime that cover an extensive range of natural and commonly used smoothing distributions.[1] We provide empirical evidence to support our claims on the CIFAR-10 dataset.

2. Preliminaries and Notation

Let h be a classifier that maps inputs from $\mathbb{R}^d$ to classes in $\mathcal{C}$. Let $\mathcal{P}$ be a (smoothing) probability distribution in $\mathbb{R}^d$. We define a *smoothed* classifier $\bar{h}$ as below:

$$\bar{h}(x) \triangleq \arg\max_{c \in \mathcal{C}} \mathbb{P}_{\Delta \sim \mathcal{P}}(h(x + \Delta) = c).$$

We refer to the process of smoothing using distribution $\mathcal{P}$ as $\mathcal{P}$-smoothing. Let $p_c(x)$ be the output probability of the base classifier for the class c. That is,

$$p_c(x) := \mathbb{P}_{\Delta \sim \mathcal{P}}(h(x + \Delta) = c).$$

Without loss of generality, we assume that $p_1(x)$ and $p_2(x)$ are the probabilities of the first and second most likely classes, respectively.

For $p > 0$, we say a smoothing distribution $\mathcal{P}$ achieves a *certified ℓ_p-norm radius* of r_p if, for a base classifier h and an input x,

$$\bar{h}(x + \delta) = \bar{h}(x), \quad \forall \delta \in \mathbb{R}^d, \|\delta\|_p \leq r_p.$$

For instance, as derived in (Cohen et al., 2019), the Gaussian smoothing distribution $\mathcal{N}(0, \sigma^2 I)$ achieves a certified 2-norm radius of $\frac{\sigma}{2}(\Phi^{-1}(p_1(x)) - \Phi^{-1}(p_2(x)))$ where Φ^{-1} is the inverse of the standard Gaussian CDF.

---

[1]We have later come to know about a concurrent work which also illustrates the difficulty of extending randomized smoothing to defend against ℓ_∞-attacks for high-dimensional data (Blum et al., 2020).

For $p_1, p_2 \in (0, 1)$, such that, $p_1 \geq p_2$, let r_p^* denote the largest r_p that can be certified using $\mathcal{P}$-smoothing for all classifiers satisfying $p_1(x) = p_1$ and $p_2(x) = p_2$. If we can show a classifier h in this class and two points $x, x' \in \mathbb{R}^d$, such that, $\bar{h}(x) \neq \bar{h}(x')$, then $r_p^* \leq \|x' - x\|_p$. We use this fact to show upper bounds on the largest p-norm radius that can be certified using a given class of distributions.

3. General i.i.d. Smoothing

We set the $\mathcal{P}$ to be a smoothing distribution $\mathcal{I}$ where each coordinate of Δ is sampled independently and identically from a symmetric distribution with zero mean, σ^2 variance with a continuous support. We prove the following theorem:

Theorem 1. *For distribution $\mathcal{I}$ and for $p_1, p_2 \in (0, 1)$, such that, $p_1 \geq 1/2$ and $p_1 + p_2 \leq 1$, the largest ℓ_p-radius r_p^* that can be certified for all classifiers satisfying $p_1(x) = p_1$ and $p_2(x) = p_2$ under $\mathcal{I}$-smoothing at input point x is bounded as:*

$$r_p^* \leq \frac{\sigma}{2\sqrt{2}d^{\frac{1}{2}-\frac{1}{p}}} \left(\frac{1}{\sqrt{1 - p_1(x)}} + \frac{1}{\sqrt{p_2(x)}} \right). \quad (2)$$

Proof. Let Z_i be the random variable modelling the ith coordinate of Δ. Define a random variable $S = \sum_{i=1}^{d} Z_i$. It is straightforward to show that this random variable is distributed symmetrically with zero mean, $d\sigma^2$ variance and a continuous support. The key intuition behind this proof is that the random variable S, which is the sum of d identical and independent random variables, will tend towards a Gaussian distribution for large values of d, making the distribution $\mathcal{I}$ suffer from some of the same limitations as the Gaussian distribution.

To simplify our analysis, we move our frame of reference so that x is at the origin. Therefore, $r_p^* \leq \|x'\|_p$. Consider a classifier g that maps points in $\{w \in \mathbb{R}^d \mid \sum_{i=1}^{d} w_i \leq s_1\}$ to class one and those in $\{w \in \mathbb{R}^d \mid \sum_{i=1}^{d} w_i \geq s_2\}$ to class two. We pick $s_1, s_2 \in \mathbb{R}^+$ such that, $\mathbb{P}(S \leq s_1) = p_1(x)$ (this requires $p_1(x) \geq 1/2$) and $\mathbb{P}(S \geq s_2) = p_2(x)$. Let x' be the point with every coordinate equal to ϵ and so, $\sum_{i=1}^{d} x'_i = \epsilon d$. Since S is symmetric and has a continuous support, $\bar{g}(x') = \bar{g}(x)$ only if $\sum_{i=1}^{d} x'_i \leq \frac{s_1 + s_2}{2}$, which implies $\epsilon \leq \frac{s_1 + s_2}{2d}$. Therefore,

$$r_p^* \leq \|x'\|_p = \epsilon d^{1/p} \leq \frac{s_1 + s_2}{2d^{1-\frac{1}{p}}}. \quad (3)$$

Figure 1 illustrates how the probabilities of the top two classes change as we move from x to x'.

Applying Chebyshev's inequality on S, we have:

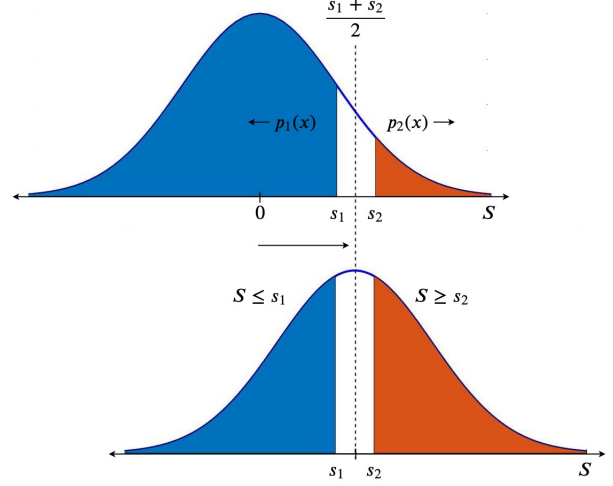$$P(S \geq s) = \frac{P(|S| \geq s)}{2} \leq \frac{d\sigma^2}{2s^2}$$

Figure 1. As the distribution of S moves from the origin to $\frac{s_1 + s_2}{2}$ the probability for class one decreases and that of class two increases. They become equal at $\frac{s_1 + s_2}{2}$ beyond which class two becomes more likely.

The value of s for which $\frac{d\sigma^2}{2s^2} = p_2(x)$ must be an upper-bound on s_2.

$$s_2 \leq \frac{\sqrt{d}\sigma}{\sqrt{2p_2(x)}}$$

Similarly, since $\mathbb{P}(S \geq s_1) = 1 - p_1(x)$,

$$s_1 \leq \frac{\sqrt{d}\sigma}{\sqrt{2(1 - p_1(x))}}$$

Substituting the above bounds for s_1 and s_2 in (3), proves Theorem (1):

$$r_p^* \leq \frac{\sigma}{2\sqrt{2}d^{\frac{1}{2}-\frac{1}{p}}} \left(\frac{1}{\sqrt{1 - p_1(x)}} + \frac{1}{\sqrt{p_2(x)}} \right).$$

$\square$

4. Generalized Gaussian Smoothing

We now restrict ourselves to the class of generalized Gaussian distributions that subsumes some commonly used and natural smoothing distributions such as Gaussian, Laplacian and uniform distributions. Using a similar approach as in the previous section, we obtain tighter upper bounds on r_p^* by restricting the smoothing distribution to generalized Gaussian. In this class of distributions, each coordinate is sampled independently from the following distribution:

$$p(z) = \frac{1}{C} e^{-(|z|/b)^q}$$

where $z \in \mathbb{R}$, $b > 0$ is the *scale parameter*, $q > 0$ is the *shape parameter* and C is the normalizing constant

$$C = \int_{-\infty}^{\infty} e^{-(|z|/b)^q} dz \tag{4}$$

$$= 2 \int_0^{\infty} e^{-z^q/b^q} dz = \frac{2b\Gamma(1/q)}{q},$$

where $\Gamma(.)$ is the gamma function. The mean of this distribution is at zero and the variance σ^2 can be calculated as

$$\sigma^2 = \frac{1}{C} \int_{-\infty}^{\infty} z^2 e^{-(|z|/b)^q} dz$$

$$= \frac{2}{C} \int_0^{\infty} z^2 e^{-z^q/b^q} dz = \frac{2b^3\Gamma(3/q)}{Cq}.$$

Substituting C from (4) leads to

$$\sigma^2 = \frac{b^2\Gamma(3/q)}{\Gamma(1/q)}.$$

Note that the class of generalised Gaussian distributions is a subset of the class of i.i.d. smoothing distributions considered in the previous section. The joint probability distribution over all the d dimensions can be expressed as:

$$p(z_1, z_2, \ldots, z_d) = \frac{1}{C^d} e^{-\sum_{i=1}^d (|z_i|/b)^q},$$

which for $q = 1, 2$ represents Laplace and Gaussian distributions, respectively. As $q \to \infty$, this distribution approximates the uniform distribution over $[-b, b]^d$. For a finite q, the level sets of the above p.d.f. define sets with constant ℓ_q-norm. Let $\mathcal{G}$ be a generalised Gaussian distribution with $q \geq 1$. The following theorem holds:

Theorem 2. *For distribution $\mathcal{G}$ and for $e^{-d/4} < p_2 \leq p_1 < 1 - e^{-d/4}$ and $p_1 + p_2 \leq 1$, the largest ℓ_p-radius r_p^* that can be certified for all classifiers satisfying $p_1(x) = p_1$ and $p_2(x) = p_2$ under $\mathcal{G}$-smoothing at input point x, is bounded as:*

$$r_p^* \leq \frac{2\sigma}{d^{\frac{1}{2}-\frac{1}{p}}} \left(\sqrt{\log(1/(1 - p_1(x)))} + \sqrt{\log(1/p_2(x))} \right) \tag{5}$$

We provide a brief proof sketch for this theorem here. As before, define random variables Z_i and S, and assume x to be at the origin. Since the above distribution satisfies all the assumptions made in the previous section, we can directly conclude that the bound in (3) holds:

$$r_p^* \leq \frac{s_1 + s_2}{2d^{1-\frac{1}{p}}}$$

From here, we strengthen our analysis by replacing Chebyshev's inequality with Chernoff bound.

$$P(S \geq s) \leq \frac{E[e^{tS}]}{e^{ts}}$$

for any $t > 0$. Since S is a sum of independent random variables $Z_1, Z_2, \ldots, Z_d$ sampled from identical distributions,

$$P(S \geq s) \leq e^{-ts} \prod_{i=1}^d E[e^{tZ_i}] \leq e^{-ts} E[e^{tZ}]^d$$

where Z is sampled from $p(z)$.

Lemma 3. *For some constant $c < 1.85$,*

$$E[e^{tZ}] \leq \sum_{m=0}^{\infty} (c^2 t^2 \sigma^2)^m$$

Proof is presented in the appendix.

Setting $t = \frac{1}{\tau\sigma\sqrt{d}}$ for some $\tau > 0$ satisfying $\frac{c^2}{\tau^2 d} < 1$, we have:

$$P(S \geq s) \leq e^{-s/\tau\sigma\sqrt{d}} \left(\sum_{m=0}^{\infty} (c^2/\tau^2 d)^m \right)^d$$

$$= \frac{e^{-s/\tau\sigma\sqrt{d}}}{(1 - \frac{c^2}{\tau^2 d})^d} \leq e^{-s/\tau\sigma\sqrt{d}} e^{4/\tau^2}$$

for $\tau^2 d \geq 16$. The value of s for which this expression is equal to $p_2(x)$ gives us the following upper-bound on s_2:

$$s_2 \leq \sigma\sqrt{d}(\tau \log(1/p_2(x)) + 4/\tau)$$

which for $\tau = 2/\sqrt{\log(1/p_2(x))}$ gives:

$$s_2 \leq 4\sigma\sqrt{d \log(1/p_2(x))}$$

and similarly, repeating the above analysis and setting $\tau = 2/\sqrt{\log(1/(1 - p_1(x)))}$, we get:

$$s_1 \leq 4\sigma\sqrt{d \log(1/(1 - p_1(x)))}$$

Both the above values for τ satisfy $\tau^2 d \geq 16$ due to the restrictions on p_1 and p_2. Substituting the above bounds for s_1 and s_2 in inequality (3), proves Theorem (2):

$$r_p^* \leq \frac{2\sigma}{d^{\frac{1}{2}-\frac{1}{p}}} \left(\sqrt{\log(1/(1 - p_1(x)))} + \sqrt{\log(1/p_2(x))} \right)$$

When $p_1(x)$ is close to one and $p_2(x)$ is close to zero, this bound is within a constant factor of the Gaussian certificate in equation (1) because $\Phi^{-1}(p)$ can be lower bounded by $\alpha\sqrt{\log(1/(1-p))} + \beta$ for some constants α and β. Figure (2) compares the behaviour of the two upper bounds, the one from i.i.d. smoothing $u_{\mathcal{I}}$ and the one from generalized Gaussian smoothing $u_{\mathcal{G}}$, with respect to the Gaussian certificate r_p obtained in equation (1). Assuming the binary classification case, for which $p_2(x) = 1 - p_1(x)$, we plot
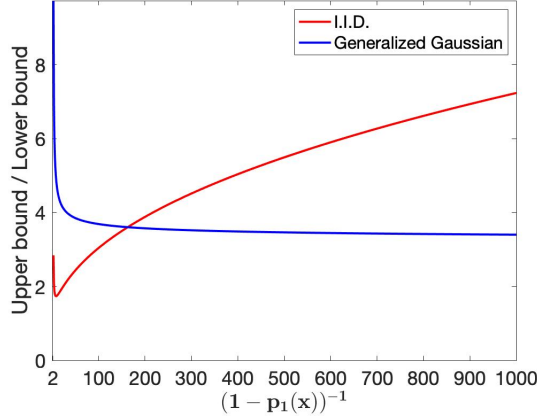
Figure 2. Comparison of the upper bounds from i.i.d. smoothing (2) and generalized Gaussian smoothing (5) w.r.t. the lower bound obtained from Gaussian smoothing (1). The x-axis represents $\frac{1}{1-p_1(x)}$ for $\frac{1}{2} \leq p_1(x) \leq 1$ and the y-axis represents the ratio of each upper bound to the Gaussian lower bound. At around $p_1(x) \approx 0.99$, the generalized Gaussian bound becomes tighter than the i.i.d. bound and gets within a constant factor of the Gaussian lower bound as $p_1(x)$ gets larger.

the ratios

$$\frac{u_{\mathcal{I}}}{r_p} = \frac{1}{\phi^{-1}(p_1(x))\sqrt{2(1-p_1(x))}},$$

$$\frac{u_{\mathcal{G}}}{r_p} = \frac{4\sqrt{\log \frac{1}{1-p_1(x)}}}{\phi^{-1}(p_1(x))}$$

which only depend on $p_1(x)$ and show that the generalized Gaussian bound is much tighter than the i.i.d. bound when $p_1(x)$ is close to one.

5. Uniform Smoothing

In this section, we analyse smoothing distributions that are uniform within a finite region around the input point x. We show stronger upper bounds for r_p^* when smoothed uniformly over ℓ_1 and ℓ_∞-norm balls. We first consider the ℓ_∞ smoothing distribution which is a limiting case for the generalized Gaussian distribution for $q = \infty$. We set $\mathcal{P}$ to be $\mathcal{U}([-b,+b]^d)$ which denotes a uniform distribution over the points in $[-b,+b]^d$.

Theorem 4. *For distribution $\mathcal{U}([-b,+b]^d)$, the largest ℓ_p-radius r_p^* that can be certified for all classifiers, is bounded as*

$$r_p^* < \frac{2b}{d^{1-\frac{1}{p}}} = 2\sqrt{3}\sigma/d^{1-\frac{1}{p}}.$$

where $\sigma^2 = b^2/3$ is the variance in each dimension.

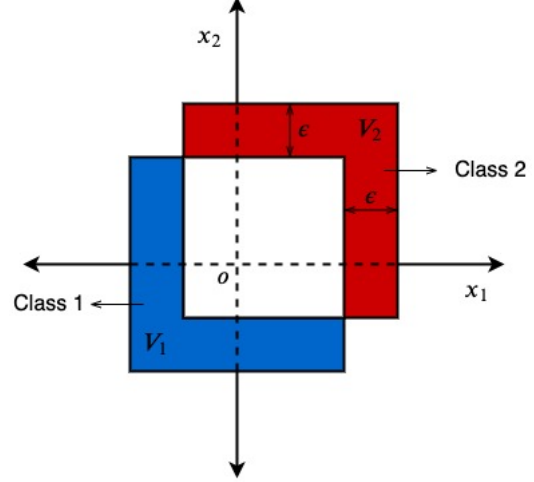*Proof.* Assume x is at origin and let x' be a point with every coordinate equal to ϵ. Let V_1 and V_2 denote the sets

Figure 3. 2-D illustration of the ℓ_∞ smoothing case. The ℓ_∞ ball is shifted by ϵ along x_1 and x_2. The points in the blue region $(V_1 - V_2)$ are mapped to class one and the points in the red region $(V_2 - V_1)$ to class two.

$[-b,+b]^d$ and $[-b+\epsilon, b+\epsilon]^d$. Consider a classifier g that maps every point in $V_1 - V_2$ to class one and every point in $V_2 - V_1$ to class two. See figure 3. Let ρ denote the probability with which the smoothing distribution for $\bar{g}(x)$ samples from $V_1 - V_2$, which is equal to the probability with which the smoothing distribution for $\bar{g}(x')$ samples from $V_2 - V_1$, or

$$\rho = \frac{(2b)^d - (2b-\epsilon)^d}{(2b)^d}$$

$$= \left(1 - \left(1 - \frac{\epsilon}{2b}\right)^d\right).$$

For $\bar{g}$ to classify x' into class one, we must have:

$$p_1(x') > p_2(x')$$
$$p_1(x) - \rho > p_2(x) + \rho$$
$$\rho < \frac{p_1(x) - p_2(x)}{2}$$
$$\left(1 - \left(1 - \frac{\epsilon}{2b}\right)^d\right) < \frac{1}{2} \qquad p_1(x) - p_2(x) \leq 1$$
$$\epsilon < 2b\left(1 - 2^{-1/d}\right) < 2b/d$$
$$\left(1 - 2^{-1/d}\right) < 1/d$$

Since $\|x'\|_p = \epsilon d^{1/p}$, the optimal radius,

$$r_p^* < 2b/d^{1-\frac{1}{p}} = 2\sqrt{3}\sigma/d^{1-\frac{1}{p}}$$

where σ^2 is the variance of $\mathcal{U}(-b,b)$. $\qquad\square$

This shows that for $p > 1$, σ (or b) needs to grow with the number of dimensions d to certify for a meaningfully large
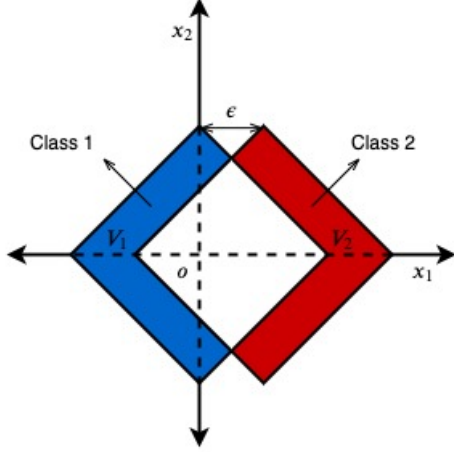
Figure 4. 2-D illustration of the ℓ_1 smoothing case. The ℓ_1 ball is shifted by ϵ along x_1. The points in the blue region ($V_1 - V_2$) are mapped to class one and the points in the red region ($V_2 - V_1$) to class two.

p-norm radius. For instance, $p = 2$ and ∞, require σ to be $\Theta(\sqrt{d})$ and $\Theta(d)$ respectively. However, since inputs can be assumed to come from $[0, 1]^d$ (possibly after some scaling and shifting of images), smoothing over distributions with such large variance may significantly lower the performance of the smoothed classifier.

We now consider the uniform ℓ_1 smoothing distribution (denoted by $\mathcal{L}_1(b)$) where points are sampled uniformly from an ℓ_1-norm ball of radius b. Note that the noise in each dimension is no longer independent.

Theorem 5. *For distribution $\mathcal{L}_1(b)$, the largest ℓ_p-radius r_p^* that can be certified for all classifiers, is bounded as*

$$r_p^* < \frac{2b}{d}.$$

The following is a proof sketch of the above theorem. Let x be at the origin and x' be the point $(\epsilon, 0, 0, \ldots, 0)$, that is, ϵ in the first coordinate and zero everywhere else. Similar to before, let V_1 and V_2 be the sets defined by the ℓ_1 balls centered at x and x' respectively.

Lemma 6. *The set $V_1 \cap V_2$ is a subset of an ℓ_1 ball of radius $b - \frac{\epsilon}{2}$.*

The proof is presented in the appendix.

As before, let g be a classifier that maps every point in $V_1 - V_2$ to class one and every point in $V_2 - V_1$ to class two (figure 4). Let ρ denote the probability with which the smoothing distribution for $\bar{g}(x)$ samples from $V_1 - V_2$, which is equal to the probability with which the smoothing
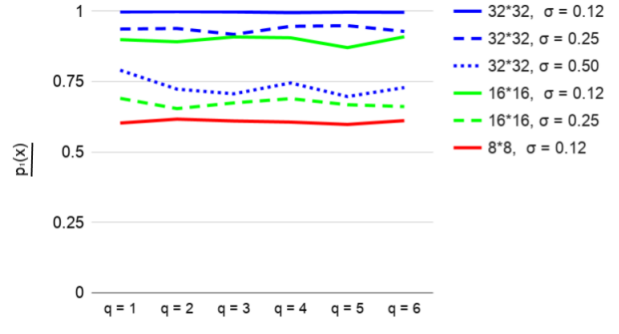

Figure 5. $p_1(x)$ for CIFAR-10 images with median certified robustness for each classifier using Generalized Gaussian smoothing for different q. For a fixed standard deviation σ, the shape of the distribution, controlled by q, has almost no effect on the likelihood that the base classifier returns the correct class.

distribution for $\bar{g}(x')$ samples from $V_2 - V_1$, or

$$\rho \geq \frac{\frac{2^d}{d!}b^d - \frac{2^d}{d!}(b - \frac{\epsilon}{2})^d}{\frac{2^d}{d!}b^d} = \left(1 - \left(1 - \frac{\epsilon}{2b}\right)^d\right).$$

We us the formula $2^d R^d / d!$ as the volume of a *d*-dimensional ℓ_1 ball of radius R. The rest of the analysis is same as that for the ℓ_∞ case and since $\|x'\|_p = \epsilon$, we have,

$$r_p^* < \frac{2b}{d},$$

which proves Theorem 5.

6. Experiments

In order to understand how our results apply to smoothing in practice, we tested the smoothed classification algorithm proposed by (Cohen et al., 2019), using Generalized Gaussian noise in each dimension, rather than Gaussian noise. We specifically tested on CIFAR-10 (32×32 pixels), as well as scaled-down versions of this dataset (16×16 and 8×8 pixels), in order to study how our bounds behave as the dimension of the input changes. Although we do not have explicit certificates for these Generalized Gaussian distributions, we are able to compare the upper bounds derived in this work for any *possible* certificates to the *actual* certificates for Gaussian smoothing on the same images. Note that we re-trained the classifier on noisy images for each noise distribution and standard deviation σ.

Note also that our main results apply specifically to smoothing based certificates which are functions of only $p_1(x)$ and $p_2(x)$ (in theory, larger certificates could be derived if more information is available to the certification algorithm). In reporting the upper bounds on possible *empirical* certificates,
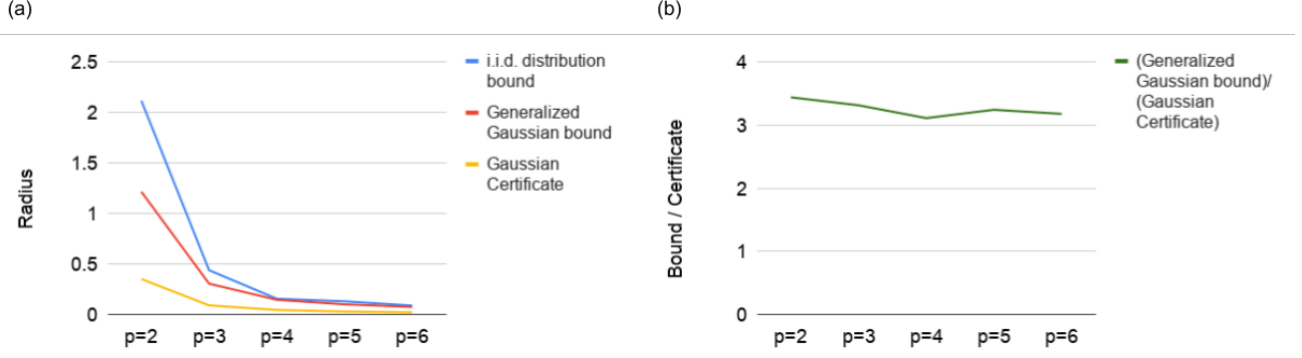
(a)

(b)

Figure 6. Upper bounds for certifying with Generalized Gaussian noise ($\sigma = .12$) on unaltered (32×32) CIFAR-10 images, with $q = p$, compared with certificates using Gaussian noise directly. At this noise level, $\underline{p_1(x)}$ is high enough for the Generalized Gaussian bound to be tighter than the i.i.d. distribution bound. Panel (a) shows the certificates and the bounds directly, while (b) shows the ratio between the tighter Generalized Gaussian bound and the certificate.
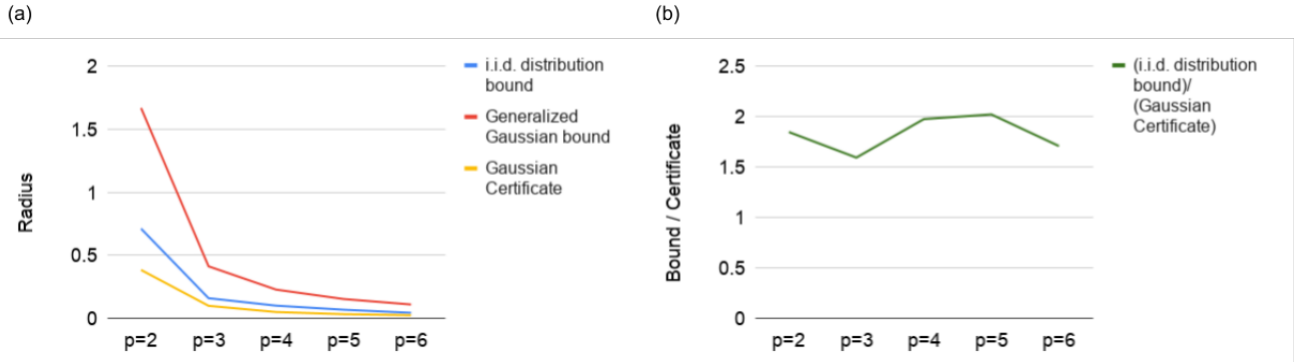
(a)

(b)

Figure 7. Repeating Figure 6 for $\sigma = .25$. At this level of noise, $\underline{p_1(x)}$ is low enough so that the i.i.d. distribution bound is tighter than the Generalized Gaussian bound (in contrast to the setup of Figure 6).

we provide the same inputs to the upper bound as we would provide to the certificate: namely, an empirical lower bound $\underline{p_1(x)}$ on $p_1(x)$, estimated from samples, and an empirical upper bound $\overline{p_2(x)}$ on $p_2(x)$. We are *not* making claims about the "optimal possible" empirical estimation procedures required to derive the largest possible certificates. We instead regard these bounds, $\underline{p_1(x)}$ and $\overline{p_2(x)}$, as *inputs* to the empirical certificate: we are only claiming that, given estimates $\underline{p_1(x)}$ and $\overline{p_2(x)}$, no certificate will exceed the computed bound. In practice, we use the estimation procedure proposed by (Cohen et al., 2019), which first selects a candidate top class label using a small number of samples, then uses a large number of samples ($100,000$ in our experiments) to compute $\underline{p_1(x)}$ based on a binomial distribution. $\overline{p_2(x)}$ is then taken as $1 - \underline{p_1(x)}$. Then, for the sake of our experiments, the only empirical input to our bound is the estimate of $\underline{p_1(x)}$.

One interesting result is that the distribution of noise added in each dimension seems to be largely irrelevant to determining $\underline{p_1(x)}$ (Figure 5). It is the variance of the noise added, *not* the specific choice of noise distribution, that determines $\underline{p_1(x)}$. This paints an even bleaker picture for the possibility of smoothing for high p-norm robustness than our theoretical results alone can: Theorems 1 and 2 still depend on $p_1(x)$ and $p_2(x)$ for the particular noise distribution used. This leaves open the possibility that certain choices of noise distributions could yield values of $p_1(x)$ large enough to counteract the scaling with p. However, empirically, we find that this is not the case: for a fixed σ, $p_1(x)$ does not depend on the shape of the smoothing distribution.

For example, one might attempt to use smoothing with $q = p$ in order to certify for the ℓ_p norm, so that the level sets of the smoothing distribution correspond to ℓ_p balls around x. This is the technique used for ℓ_1 certification by (Lécuyer et al., 2019), and for ℓ_2 certification by (Cohen
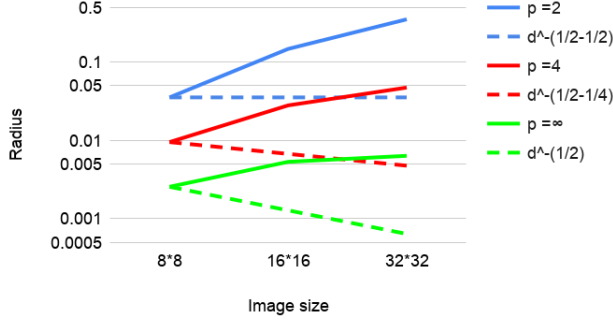
Figure 8. Certified Radius at different resolutions of CIFAR-10 using Gaussian noise ($\sigma = .12$). The increase in accuracy of the base classifier on higher-resolution images overcomes the inverse scaling with d in Eq. 1, achieving higher certified radii. Solid lines represent actual certificates and dashed lines represent how the certificates would scale if $p_1(x)$ remained constant as resolution increased.
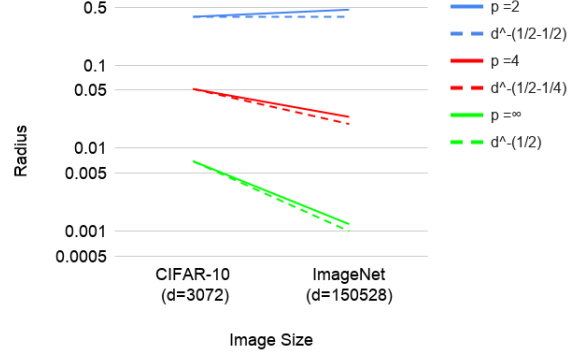
Figure 9. Certified Radius using Gaussian noise ($\sigma = .25$), for datasets of different image resolutions. We see that for $p > 2$, the certificates (solid lines) decrease with higher dimensionality almost as quickly as one would expect from the explicit dependence on d in Equation 1 (dashed lines).

et al., 2019). However, we find (Figures 6, 7) that, as anticipated by Figure 2, for $p > 2$, this can only achieve at best a constant factor improvement in certified robustness compared to simply using Gaussian smoothing with the certificate from (Cohen et al., 2019) and applying equivalence of norms (Equation 1). Note that, as shown in Figure 5, it was *only* for the lowest level of noise tested ($\sigma = .12$) and the highest resolution images tested (32×32) that $p_1(x)$ was sufficiently close to 1 for the Generalized Gaussian bound to be tighter than the i.i.d. distribution bound (Figure 6). For all other configurations (Figure 7, other plots are given in supplementary materials) the i.i.d. bound is tighter.

In the case of Gaussian smoothing, (Cohen et al., 2019) makes an argument that, as image resolution increases, the base classifier will become more tolerant to noise, because information will be redundantly encoded in the additional pixels. This should allow us to increase the magnitude of the smoothing variance σ^2 proportionally to d. It is because by average-pooling back down a large image to a low-resolution one, the variance in each pixel of the smaller image will decrease proportionally with d. Then, if it is possible to classify noisy images at the lower resolution with a certain accuracy $p_1(x)$, it should be possible to classify images at the higher resolution with higher levels of noise. This increase in the amount of noise that can be added to high resolution images (to obtain roughly the same accuracy to that of low resolution ones) will cancel out the decrease in the robustness radius due to the curse of dimensionality explained in this paper. It is because based on Equation 1, if σ is allowed to scale with $\sqrt{d}$ with $p_1(x)$ and $p_2(x)$ unchanged, then the certified radius should even remain constant with d in the ℓ_∞ case.

For image datasets that are *identical* except for a scaling factor, we observe a related phenomenon: for a fixed noise variance, $p_1(x)$ tends to increase with the resolution of the image (i.e., the dimensionality of the input), and therefore the certified radii tend to increase with d in the $p = 2$ case. In Figure 8, we show that, for $p > 2$, this increase is enough to counteract the *inverse* scaling with d in Equation 1, at least in the case of low-resolution CIFAR-10 images. In other words, we still get larger certificates for larger-resolution images, simply because our base classifier becomes more accurate on noisy images as resolution increases. We emphasize that this is using the standard Gaussian noise: we have demonstrated that other i.i.d distributions will not give significantly better certificates.

The above setup, however, is an artificial scenario. In the real world, higher-resolution datasets are typically used for classification tasks which could *not* be accomplished with high accuracy at a lower resolution. As shown in Figure 9, if we compare, for a fixed σ, a real-world low dimensional classification task (CIFAR-10, $d = 3072$) to a high dimensional classification task (ImageNet, $d = 150528$), we see that the certified radius (and therefore $p_1(x)$), does *not* substantially increase with higher resolution. Therefore, for higher p-norms, the certified radius decreases with dimension with a scaling nearly as extreme as the explicit $d^{(1/2-1/p)}$ factor in Equation 1. Therefore, in practice, the curse of dimensionality can be observed as explained in this paper and it cannot be overcome using a novel choice of i.i.d. smoothing distribution.

7. Conclusion

In this work, we demonstrated some limitations of common smoothing distributions for ℓ_p-norm bounded adversaries when $p > 2$. We partially answer the question, raised in (Cohen et al., 2019), whether smoothing techniques similar to Gaussian smoothing can be employed to achieve certifiable robustness guarantees for a general ℓ_p-norm bounded adversary. Most i.i.d. smoothing distributions fail to yield good robustness guarantees in the high-dimensional regime against ℓ_p-norm bounded attacks when $p > 2$. Their performance is no better than that of Gaussian smoothing up to a constant factor. While a constant factor improvement in performance could be critical in certain applications, the focus of this work is on the effect of dimensionality on certified robustness. We note that, in our analysis, we focus on i.i.d. and symmetric smoothing distributions. Our analysis highlights the importance of developing input-dependent smoothing techniques rather than the current smoothing methods based on i.i.d. distributions.

Software and Data

The code for our experiments is available on GitHub at:

https://github.com/alevine0/smoothingGenGaussian

References

Athalye, A., Carlini, N., and Wagner, D. Obfuscated gradients give a false sense of security: Circumventing defenses to adversarial examples. In Dy, J. and Krause, A. (eds.), *Proceedings of the 35th International Conference on Machine Learning*, volume 80 of *Proceedings of Machine Learning Research*, pp. 274–283, Stockholmsmssan, Stockholm Sweden, 10–15 Jul 2018. PMLR.

Blum, A., Dick, T., Manoj, N., and Zhang, H. Random smoothing might be unable to certify ℓ_∞ robustness for high-dimensional images. *CoRR*, abs/2002.03517, 2020.

Buckman, J., Roy, A., Raffel, C., and Goodfellow, I. J. Thermometer encoding: One hot way to resist adversarial examples. In *6th International Conference on Learning Representations, ICLR 2018, Vancouver, BC, Canada, April 30 - May 3, 2018, Conference Track Proceedings*, 2018.

Carlini, N. and Wagner, D. A. Adversarial examples are not easily detected: Bypassing ten detection methods. In *Proceedings of the 10th ACM Workshop on Artificial Intelligence and Security, AISec@CCS 2017, Dallas, TX, USA, November 3, 2017*, pp. 3–14, 2017.

Chiang, P.-y., Ni, R., Abdelkader, A., Zhu, C., Studer, C., and Goldstein, T. Certified defenses for adversarial patches. In *8th International Conference on Learning Representations*, 2020.

Cohen, J., Rosenfeld, E., and Kolter, Z. Certified adversarial robustness via randomized smoothing. In Chaudhuri, K. and Salakhutdinov, R. (eds.), *Proceedings of the 36th International Conference on Machine Learning*, volume 97 of *Proceedings of Machine Learning Research*, pp. 1310–1320, Long Beach, California, USA, 09–15 Jun 2019. PMLR.

Dhillon, G. S., Azizzadenesheli, K., Lipton, Z. C., Bernstein, J., Kossaifi, J., Khanna, A., and Anandkumar, A. Stochastic activation pruning for robust adversarial defense. In *6th International Conference on Learning Representations, ICLR 2018, Vancouver, BC, Canada, April 30 - May 3, 2018, Conference Track Proceedings*, 2018.

Gong, Z., Wang, W., and Ku, W. Adversarial and clean data are not twins. *CoRR*, abs/1704.04960, 2017.

Goodfellow, I. J., Shlens, J., and Szegedy, C. Explaining and harnessing adversarial examples. In *3rd International Conference on Learning Representations, ICLR 2015, San Diego, CA, USA, May 7-9, 2015, Conference Track Proceedings*, 2015.

Grosse, K., Manoharan, P., Papernot, N., Backes, M., and McDaniel, P. D. On the (statistical) detection of adversarial examples. *CoRR*, abs/1702.06280, 2017.

Guo, C., Rana, M., Cissé, M., and van der Maaten, L. Countering adversarial images using input transformations. In *6th International Conference on Learning Representations, ICLR 2018, Vancouver, BC, Canada, April 30 - May 3, 2018, Conference Track Proceedings*, 2018.

Laidlaw, C. and Feizi, S. Functional adversarial attacks. In Wallach et al. (2019), pp. 10408–10418.

Lécuyer, M., Atlidakis, V., Geambasu, R., Hsu, D., and Jana, S. Certified robustness to adversarial examples with differential privacy. In *2019 IEEE Symposium on Security and Privacy, SP 2019, San Francisco, CA, USA, May 19-23, 2019*, pp. 656–672, 2019.

Lee, G., Yuan, Y., Chang, S., and Jaakkola, T. S. Tight certificates of adversarial robustness for randomly smoothed classifiers. In Wallach et al. (2019), pp. 4911–4922.

Levine, A. and Feizi, S. Wasserstein smoothing: Certified robustness against wasserstein adversarial attacks. In Chiappa, S. and Calandra, R. (eds.), *The 23rd International Conference on Artificial Intelligence and Statistics, AISTATS 2020, 26-28 August 2020, Online [Palermo, Sicily, Italy]*, volume 108 of *Proceedings of Machine Learning Research*, pp. 3938–3947. PMLR, 2020a.

Levine, A. and Feizi, S. (de)randomized smoothing for certifiable defense against patch attacks. *CoRR*, abs/2002.10733, 2020b.

Levine, A. and Feizi, S. Robustness certificates for sparse adversarial attacks by randomized ablation. In *The Thirty-Fourth AAAI Conference on Artificial Intelligence, AAAI 2020, The Thirty-Second Innovative Applications of Artificial Intelligence Conference, IAAI 2020, The Tenth AAAI Symposium on Educational Advances in Artificial Intelligence, EAAI 2020, New York, NY, USA, February 7-12, 2020*, pp. 4585–4593. AAAI Press, 2020c.

Li, B., Chen, C., Wang, W., and Carin, L. Certified adversarial robustness with additive noise. In *Advances in Neural Information Processing Systems 32: Annual Conference on Neural Information Processing Systems 2019, NeurIPS 2019, 8-14 December 2019, Vancouver, BC, Canada*, pp. 9459–9469, 2019.

Li, X. and Li, F. Adversarial examples detection in deep networks with convolutional filter statistics. In *IEEE International Conference on Computer Vision, ICCV 2017, Venice, Italy, October 22-29, 2017*, pp. 5775–5783, 2017.

Madry, A., Makelov, A., Schmidt, L., Tsipras, D., and Vladu, A. Towards deep learning models resistant to adversarial attacks. In *6th International Conference on Learning Representations, ICLR 2018, Vancouver, BC, Canada, April 30 - May 3, 2018, Conference Track Proceedings*, 2018.

Raghunathan, A., Steinhardt, J., and Liang, P. Semidefinite relaxations for certifying robustness to adversarial examples. In *Proceedings of the 32nd International Conference on Neural Information Processing Systems*, NIPS18, pp. 1090010910, Red Hook, NY, USA, 2018. Curran Associates Inc.

Salman, H., Li, J., Razenshteyn, I. P., Zhang, P., Zhang, H., Bubeck, S., and Yang, G. Provably robust deep learning via adversarially trained smoothed classifiers. In *Advances in Neural Information Processing Systems 32: Annual Conference on Neural Information Processing Systems 2019, NeurIPS 2019, 8-14 December 2019, Vancouver, BC, Canada*, pp. 11289–11300, 2019.

Shafahi, A., Huang, W. R., Studer, C., Feizi, S., and Goldstein, T. Are adversarial examples inevitable? In *7th International Conference on Learning Representations, ICLR 2019, New Orleans, LA, USA, May 6-9, 2019*. OpenReview.net, 2019.

Singla, S. and Feizi, S. Robustness certificates against adversarial examples for relu networks. *CoRR*, abs/1902.01235, 2019.

Singla, S. and Feizi, S. Second-order provable defenses against adversarial attacks. *International Conference on Machine Learning (ICML)*, 2020.

Szegedy, C., Zaremba, W., Sutskever, I., Bruna, J., Erhan, D., Goodfellow, I. J., and Fergus, R. Intriguing properties of neural networks. In *2nd International Conference on Learning Representations, ICLR 2014, Banff, AB, Canada, April 14-16, 2014, Conference Track Proceedings*, 2014.

Teng, J., Lee, G.-H., and Yuan, Y. ℓ_1 adversarial robustness certificates: a randomized smoothing approach, 2020.

Uesato, J., O'Donoghue, B., Kohli, P., and van den Oord, A. Adversarial risk and the dangers of evaluating against weak attacks. In *Proceedings of the 35th International Conference on Machine Learning, ICML 2018, Stockholmsmässan, Stockholm, Sweden, July 10-15, 2018*, pp. 5032–5041, 2018.

Wallach, H. M., Larochelle, H., Beygelzimer, A., d'Alché-Buc, F., Fox, E. B., and Garnett, R. (eds.). *Advances in Neural Information Processing Systems 32: Annual Conference on Neural Information Processing Systems 2019, NeurIPS 2019, 8-14 December 2019, Vancouver, BC, Canada*, 2019.

Wong, E. and Kolter, J. Z. Provable defenses against adversarial examples via the convex outer adversarial polytope. In *Proceedings of the 35th International Conference on Machine Learning, ICML 2018, Stockholmsmässan, Stockholm, Sweden, July 10-15, 2018*, pp. 5283–5292, 2018.

Zhang, D., Ye, M., Gong, C., Zhu, Z., and Liu, Q. Black-box certification with randomized smoothing: A functional optimization based framework. *CoRR*, abs/2002.09169, 2020.

A. Proof for lemma 3

Proof. Applying the series expansion of e^{tZ}, we get,

$$E[e^{tZ}] = \sum_{n=0}^{\infty} \frac{t^n E[Z^n]}{n!}$$

$$E[Z^n] = \frac{1}{C} \int_{-\infty}^{\infty} z^n e^{-(|z|/b)^q} dz$$

$$= \frac{1}{C} \int_0^{\infty} (1 + (-1)^n) z^n e^{-z^q/b^q} dz$$

$$= \begin{cases} 0, & n \text{ is odd} \\ \frac{2}{C} \int_0^{\infty} z^n e^{-z^q/b^q} dz, & n \text{ is even} \end{cases}$$

When n is even:

$$E[Z^n] = \frac{2}{C} \int_0^{\infty} z^n e^{-z^q/b^q} dz$$

$$= \frac{2b^{n+1} \Gamma\left(\frac{n+1}{q}\right)}{Cq}$$

Substituting C,

$$E[Z^n] = \frac{b^n \Gamma\left(\frac{n+1}{q}\right)}{\Gamma(1/q)} \leq b^n \Gamma(n+1) \qquad \text{for } q \geq 1$$

$$E[Z^n] \leq b^n n!$$

Therefore, keeping only the terms with even n in the expansion of $E[e^{tZ}]$, we get:

$$E[e^{tZ}] \leq \sum_{m=0}^{\infty} (t^2 b^2)^m$$

$$= \sum_{m=0}^{\infty} \left(\frac{t^2 \sigma^2 \Gamma(1/q)}{\Gamma(3/q)}\right)^m \qquad \text{using } \sigma^2 = \frac{b^2 \Gamma(3/p)}{\Gamma(1/p)}$$

$$\leq \sum_{m=0}^{\infty} (c^2 t^2 \sigma^2)^m$$

for some positive constant $c < 1.85$, because,

$$\frac{\Gamma(1/q)}{\Gamma(3/q)} = \frac{3q\Gamma(1 + 1/q)}{q\Gamma(1 + 3/q)} \qquad \text{(using } \Gamma(z+1) = z\Gamma(z))$$

$$= \frac{3\Gamma(1 + 1/q)}{\Gamma(1 + 3/q)}$$

$$< 1.85^2$$

(for $q \geq 1$, $\Gamma(1 + 1/q) \leq 1$ and $\Gamma(1 + 3/q) > 0.88$)

$\square$

B. Proof for lemma 6

Proof. The points in V_1 satisfy the following 2^d constraints:

$$x_1 + x_2 + \cdots + x_d \leq b$$
$$-x_1 + x_2 + \cdots + x_d \leq b$$
$$x_1 - x_2 + \cdots + x_d \leq b$$
$$-x_1 - x_2 + \cdots + x_d \leq b$$
$$\vdots$$
$$-x_1 - x_2 - \cdots - x_d \leq b$$

Similarly, points in V_2 satisfy,

$$(x_1 - \epsilon) + x_2 + \cdots + x_d \leq b$$
$$-(x_1 - \epsilon) + x_2 + \cdots + x_d \leq b$$
$$(x_1 - \epsilon) - x_2 + \cdots + x_d \leq b$$
$$-(x_1 - \epsilon) - x_2 + \cdots + x_d \leq b$$
$$\vdots$$
$$-(x_1 - \epsilon) - x_2 - \cdots - x_d \leq b$$

Then, the points in $V_1 \cap V_2$ must satisfy the following set of constraints constructed by picking constraints that have a $+$ sign for x_1 in the first set of constraints and a $-$ sign for x_1 in the second set.

$$x_1 + x_2 + \cdots + x_d \leq b$$
$$-(x_1 - \epsilon) + x_2 + \cdots + x_d \leq b$$
$$x_1 - x_2 + \cdots + x_d \leq b$$
$$-(x_1 - \epsilon) - x_2 + \cdots + x_d \leq b$$
$$\vdots$$
$$-(x_1 - \epsilon) - x_2 - \cdots - x_d \leq b$$

They may be rewritten as,

$$(x_1 - \epsilon/2) + x_2 + \cdots + x_d \leq b - \epsilon/2$$
$$-(x_1 - \epsilon/2) + x_2 + \cdots + x_d \leq b - \epsilon/2$$
$$(x_1 - \epsilon/2) - x_2 + \cdots + x_d \leq b - \epsilon/2$$
$$-(x_1 - \epsilon/2) - x_2 + \cdots + x_d \leq b - \epsilon/2$$
$$\vdots$$
$$-(x_1 - \epsilon/2) - x_2 - \cdots - x_d \leq b - \epsilon/2$$

which define an ℓ_1 ball of radius $b - \epsilon/2$ centered at $(\epsilon/2, 0, \ldots, 0)$, that is, $\epsilon/2$ in the first coordinate and zero everywhere else.

$\square$

C. Additional Plots of Certificate Upper Bounds

See Figure 10.

D. Experimental Details

Our experiments are adapted from the released code for ℓ_2 smoothing from (Cohen et al., 2019). In particular, for each Generalized Gaussian distribution with varying parameter q and standard deviation σ, we trained a ResNet-110 classifier on CIFAR-10 for 90 epochs, with the training under the same noise distribution as used for certification. All training and certification parameters are identical to those used in (Cohen et al., 2019) unless otherwise specified. In particular, all certificates are reported to 99.9% confidence, and we tested using a 500-image subset of the CIFAR-10 test set. For lower-resolution versions of CIFAR-10, we again trained separate models for each resolution used, with the resolution at training time matching the resolution at test time. We first reduced the image resolutions before adding noise, then, once the noise was added, scaled the images back to the original 32×32 resolution (by repeating pixel values) before classifying with ResNet-110: this ensured that the number of parameters did not vary between classifiers.

We trained with $\sigma = 0.12, 0.25, 0.50, 1.00$ for resolutions 32×32, 16×16 and 8×8. At higher levels of noise for each scale ($\sigma = 0.25$ for 8×8, $\sigma = 0.5$ for 8×8 and 16×16, $\sigma = 1.00$ on all scales) the resulting classifiers could not correctly certify the median image ($p_1(x) < .5$), so we do not report any certificates.

Values for ImageNet for the median certificate under Gaussian noise are adapted from the released certificate data from (Cohen et al., 2019).
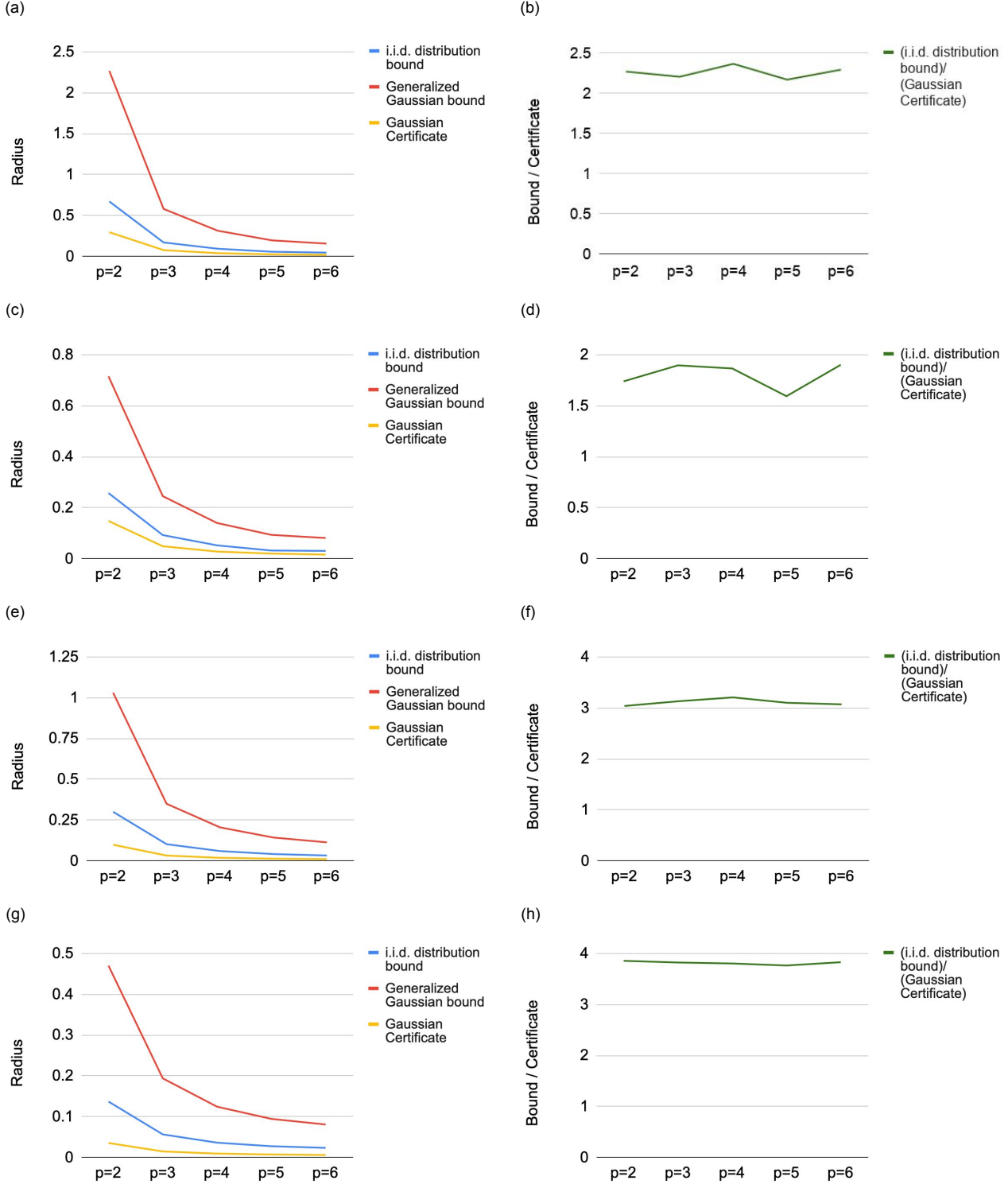
(a)

(b)

(c)

(d)

(e)

(f)

(g)

(h)

Figure 10. Upper bounds for certifying with Generalized Gaussian noise on CIFAR-10 images, with $q = p$, compared with certificates using Gaussian noise directly. Left panels show the certificates and the bounds directly, while right panels show the ratios between the i.i.d. distribution bounds (tighter in each case) and the certificates. Panels (a,b) use unaltered CIFAR-10 images with $\sigma = 0.5$ noise. Panels (c,d) and (e,f) use CIFAR-10 images at 16×16 scale with $\sigma = 0.12$ and $\sigma = 0.25$ respectively. Panels (g,h) use CIFAR-10 images at 8×8 scale with $\sigma = 0.12$.